Journal of Hazardous Materials 162 (2009) 80–91

Contents lists available at ScienceDirect

Journal of Hazardous Materials

journal homepage: www.elsevier.com/locate/jhazmat

Long-term leaching from MSWI air-pollution-control residues: Leaching characterization and modeling

Jiri Hyks*, Thomas Astrup, Thomas H. Christensen

Technical University of Denmark, Department of Environmental Engineering, Building 115, 2800 Lyngby, Denmark

ARTICLE INFO

Article history:
Received 17 December 2007
Received in revised form 7 March 2008
Accepted 5 May 2008
Available online 9 May 2008

Keywords:
Air-pollution-control residues
Leaching
Heavy metals
Oxyanions
Modeling

ABSTRACT

Long-term leaching of Ca, Fe, Mg, K, Na, S, Al, As, Ba, Cd, Co, Cr, Cu, Hg, Mn, Ni, Pb, Zn, Mo, Sb, Si, Sn, Sr, Ti, V, P, Cl, and dissolved organic carbon from two different municipal solid waste incineration (MSWI) air-pollution-control residues was monitored during 24 months of column percolation experiments; liquid-to-solid (L/S) ratios of 200–250 L/kg corresponding to more than 10,000 years in a conventional landfill were reached. Less than 2% of the initially present As, Cu, Pb, Zn, Cr, and Sb had leached during the course of the experiments. Concentrations of Cd, Fe, Mg, Hg, Mn, Ni, Co, Sn, Ti, and P were generally bellow 1 μg/L; overall less than 1% of their mass leached. Column leaching data were further used in a two-step geochemical modeling in PHREEQC in order to (i) identify solubility controlling minerals and (ii) evaluate their interactions in a water-percolated column system over L/S of 250 L/kg. Adequate predictions of pH, alkalinity, and the leaching of Ca, S, Al, Si, Ba, and Zn were obtained in a simultaneous calculation. Also, it was suggested that removal of Ca and S together with depletion of several minerals apparently caused dissolution of ettringite-like phases. In turn, significant increase in leaching of oxyanions (especially Sb and Cr) was observed at late stage of leaching experiments.

1. Introduction

Municipal solid waste incineration (MSWI) with energy recovery is one of today's major technologies to deal with increasing amounts of municipal solid waste. Necessary cleaning of flue gases however generates an additional stream of residues, i.e. air-pollution-control (APC) residues [1]. In Denmark, about 90,000 metric tons of APC residues are annually produced from approximately 3,000,000 metric tons of municipal solid waste [2]. APC residues contain high concentrations of different pollutants which make them potentially hazardous [3,4]; therefore, APC residues are often landfilled or stored underground after various kinds of pre-treatment.

The main concern with respect to utilization and/or landfilling of MSWI residues is the release of elements (e.g. salts and heavy metals) when in contact with water, i.e. leaching. In order to avoid contamination of the environment and, more recently, also to provide an adequate input for a life-cycle assessment of these residues, the leaching of salts and metals should be quantified prior to any utilization [5,6]. Further, this quantification needs to be done both in a short- and long-term perspective to include both immediate and end-of-life impacts. Short-term leaching quantification (<100 years) may be done using leaching data, both laboratory and full-scale, often combined with geochemical modeling [7,8]. Long-term leaching quantifications (centuries to millennia) on the other hand, rely largely on forward modeling as even accelerated laboratory test cannot provide the full dataset. However, some input data are still necessary to set-up and validate a model. It should be realized that analyses of the total composition does not provide adequate information as no direct relationship between material composition and leaching has been shown for most elements [9]. Hence, a description of the actual leaching behavior determined by leaching experiments is preferred.

Despite the differences in solid composition and structural properties, it is generally accepted that leaching from both major types of MSWI residues (i.e. bottom ashes and APC residues) is governed by the following processes: dissolution/precipitation of minerals, (in)organic complexation, and sorption on reactive surfaces [10–12]. Consequently, three groups of elements can be distinguished based on predominant leaching behavior: availability-controlled elements, solubility-controlled elements, and complexation/sorption-controlled elements (please refer to Section 3 for further details). Various combinations of the above controlling processes occur due to competition and the overall leaching control for a given element may thus vary in time. Nevertheless, leaching of many elements is usually expected to decrease with time. This assumption is largely based on observations from

* Corresponding author. Tel.: +45 4525 1498; fax: +45 4593 2850.
E-mail address: jrh@env.dtu.dk (J. Hyks).

0304-3894/$ – see front matter © 2008 Elsevier B.V. All rights reserved.
doi:10.1016/j.jhazmat.2008.05.011

Nomenclature

akermanite	Ca_2MgSiO_7
anhydrite	$CaSO_4$
barite	$BaSO_4$
calcite	$CaCO_3$
diaspore	AlOOH
ettringite	$Ca_6Al_2(SO_4)_3(OH)_{12}\cdot 32H_2O$
Friedel's salt	$Ca_4Al_2Cl_2(OH)_{12}\cdot 4H_2O$
gypsum	$CaSO_4\cdot 2H_2O$
halite	NaCl
hydrophilite	$CaCl_2$
lime	CaO
monosulphate	$Ca_4Al_2O_6(SO_4)\cdot 6H_2O$
portlandite	$Ca(OH)_2$
powellite	$CaMoO_4$
strätlingite	$Ca_2Al_2(SiO_2)(OH)_{10}\cdot 3H_2O$
sylvite	KCl
willemite	Zn_2SiO_4
zincite	ZnO
"Cr-ettringite"	$Ca_6Al_2(CrO_4)_3(OH)_{12}\cdot 26H_2O$

relatively short-term leaching experiments with bottom ashes [8,13]. However, even though bottom ashes are likely comparable with APC residues from the leaching-control point-of-view, differences exist. APC residues have much higher "natural" pH, alkalinity, and total content of metals and readily soluble salts [14,15] while the DOC content is lower [1]. This makes APC residues less "stable" from a leaching point of view. Moreover, long-term leaching data for APC residues are de facto unavailable due to their treatment options (e.g. landfills, back-filling of mines). Full-scale leaching data for a period of up to 20 years can sometimes be obtained in case of a landfill [16]. However, such landfills most often contain other waste types as well thereby making it impossible to "isolate" leaching from the APC residues. Twenty years of leaching often corresponds to a liquid-to-solid (L/S) ratio less then 1 L/kg (please refer to Section 3 for further details). In standardized laboratory percolation experiments, L/S 10 L/kg is usually an end-point [8,17]. Such low-L/S-ratio data are not suited for long-term leaching predictions because only a small fraction of even major elements leach within L/S 10 L/kg. Thus, potentially important processes (e.g. depletion of controlling mineral phase) may be overlooked. In other words, only a minor fraction of the total pollution potential from APC residues is described by current research. This limited knowledge is insufficient for setting up and validating leaching prediction models focusing on evaluating the long-term environmental consequences of utilizing or landfilling of APC residues.

The objectives of this paper are: (i) to provide an insight in long-term leaching from two types of APC residues based on high-resolution percolation data, (ii) to identify and explain the overall controlling processes by means of geochemical modeling, and finally (iii) to investigate possible depletion of elements during the long-term experiments.

2. Experimental

2.1. Residue samples

Two APC residues collected at different Danish MSWI plants were used; both materials will be referred to as "residues" unless noted otherwise. The first residue was a "pure" fly ash without added lime and the acid–gas neutralization products; it was collected in an electrostatic precipitator. Herein, this residue will be referred to as the "FA-residue". The latter material was a semi-dry APC residue, i.e. a mixture of fly ash, unreacted lime, and acid–gas neutralization products collected in a baghouse filter. Analogically, it will be referred to as the "SD-residue". In agreement with Chandler et al. [1] both FA- and SD-residue were very fine, dusty materials with particles smaller than 1 mm and moisture contents of 1.2% and 4.7%, respectively. Elemental composition was determined by inductively coupled plasma atomic emission spectrometry (ICP-AES) after total digestion in $HCl/HF/HNO_3$ (Table 1). Chloride (Cl) and bromide (Br) were determined using X-ray fluorescence (XRF) on non-digested subsamples. The FA-residue was characterized by lower pH and higher amounts of pollutants than the SD-residue. This is primarily because contaminants in the SD-residue are "diluted" with unreacted lime and neutralization products.

Table 1
Elemental composition of untreated residues determined by ICP-AES after microwave assisted digestion with $HCl/HF/HNO_3$

Element		FA		SD	
DM[a]	%	98.8		95.3	
Al	g/kg	35.7	±0.4	18.3	±0.2
Si	g/kg	90	±2	63	±2
Ca	g/kg	181	±3	331	±3
Fe	g/kg	13.8	±0.2	9.7	±0.1
Mg	g/kg	14.1	±2	7.8	±1
K	g/kg	50	±2	17.1	±1
Na	g/kg	42.3	±1	16	±1
As	mg/kg	380	±50	80	±20
Ba	mg/kg	1120	±70	620	±40
Cd	mg/kg	240	±40	100	±17
Cr (total)	mg/kg	700	±80	200	±25
Ni	mg/kg	67.4	±9	37.5	±5
Cu	mg/kg	1170	±160	500	±70
Mo	mg/kg	28	±5	9	±2
Sb	mg/kg	1170	±90	340	±40
Zn	g/kg	31.7	±4	9.1	±1.3
Pb	g/kg	6.8	±0.9	2.1	±0.3
S	g/kg	57	±2	35	±2
Sr	mg/kg	400	±27	500	±34
P	g/kg	10	±1	3.4	±0.2
Cl[b]	g/kg	122	±4	173	±5
Br[b]	mg/kg	1400	±15	900	±10

[a] Determined after drying 500 g of material at 105 °C.
[b] Determined using XRF on non-digested subsample.

2.2. Column experiments

Residues were subjected to percolation experiments based on the CEN/TS 14405 [17]. In order to obtain long-term leaching data, standardized experiments were extended over 24 months. L/S ratios of 207 L/kg and 245 L/kg were reached for the FA- and the SD-residue, respectively. This corresponded to more than 10,000 years in a typical landfill. A longer leaching period was the only deviation from the standardized procedure as flow velocity was maintained between 10–14 mL/h. Plexiglass columns with an inner diameter of 50 mm and length of 300 mm were used. All other equipment was made of either high-density polyethylene or glass and rinsed in a weak solution of HNO_3 (p.a.) before use. Laboratory routine consisted of several operations: filling the columns, equilibration, sampling of eluates, and sample treatment. First, a thin layer of acid-washed sand was placed at the bottom of the column. Residues were then added in successive layers (20–30 mm each) and gently compacted with a rammer. The total height of residues in column was about 280 mm. Another layer of acid-washed sand was added at the top of the column. Saturation was done from the bottom of each column in the way that eluent (i.e. distilled water stored in an open-air container) was allowed to slowly soak into the column using a difference in hydrostatic pressure between the column and

the container with eluent. After the column was fully saturated, one week of leachate recirculation ensured the initial equilibration; for details we refer to the CEN/TS 14405 procedure. Thereafter, more eluent was introduced to the column in an up-flow direction at the flow rate of 10–14 mL/h. The "equilibrated" leachate corresponding to L/S 0.1 L/kg was collected from the outlet at the top of the column. Leachate samples were then taken frequently to avoid large sample volumes that would average the measured solution concentrations.

2.3. Leachate treatment

Leachates were filtrated through 0.45 μm polypropylene filters; pH and conductivity were measured immediately after filtration. Filtrates were then split in two sub-samples; one was acidified with HNO_3 (p.a.) and used to determine the solution concentrations of Ca, S, Fe, Mg, K, Na, Al, As, Ba, Cd, Co, Cr, Cu, Hg, Mn, Ni, Pb, Zn, Mo, Sb, Si, Sn, Sr, Ti, V, and P by ICP-AES. It was assumed that S and P measured by ICP-AES equalled to SO_4^{2-} and PO_4^{2-} respectively. The non-acidified fraction was used to determine concentrations of chloride and DOC by ion chromatography and carbon analyzer, respectively. Moreover, total alkalinity was determined by titration with 0.1 M H_2SO_4 (p.a.) to an end-point at pH 4.5.

2.4. Removal of elements

Removal of elements during the leaching experiments was calculated from their leaching curves using cumulative Simpson's integration with uneven spacing [18].

2.5. Modeling of solubility controlling minerals

Minerals which may possibly control leaching of major elements were identified according to the approach of Meima and Comans [10]. Speciation of eluate samples was calculated in PHREEQC [19] assuming oxidizing conditions (pH + pe = 15); pH was fixed at value measured in eluates. The thermodynamic database used by Astrup et al. [7] was amended with new phases given in Table 2.

Generally, analytically determined concentrations of all elements were entered as components in solution and saturation indices (SI) for all minerals included in the database were calculated. This way, an indication of whether a given mineral is precipitated or close to equilibrium under the solution conditions was obtained. Minerals with $-1 < SI < +1$ were considered to be the potential solubility controlling minerals. The occurrence of those minerals under the experimental conditions was cross-checked with recent mineralogy studies [15,20–23]. It should be noted that ionic strength (I) of the initial few leachate samples was $I > 4$ for both the FA- and the SD-column. This is outside the scope of the Davies equation used in PHREEQC to calculate activity coefficients; however, in our previous study [12] we have shown that using the Pitzer equation did not result in the prediction of different solubility controlling minerals, and that the limited range of thermodynamic data available for the Pitzer equation made this approach impractical for calculating activity coefficients of such complex systems. Further, the ionic strength decreased rapidly with removal of salts (i.e. within L/S 2 L/kg) after which the Davies equation was fully applicable. On this basis, we have chosen to use the Davies equation to calculate activity coefficients for all eluate samples.

2.6. Percolation modeling

2.6.1. General description of the scenario

Results of the solubility-control modeling for Ca, S, Al, Si, Ba, and Zn in the SD-column were further evaluated using a simple percolation scenario in PHREEQC; pH and alkalinity were modeled as well. In order to do this, 1 kg of a hypothetical initial mineral assemblage containing a number of solubility controlling minerals was created. This initial assemblage contained the above elements and was derived (discussed later) from the total composition shown in Table 1. A one-cell column containing the mineral assemblage was set-up and distilled water equilibrated with atmospheric CO_2 (open-air tank; pH ~5.6) was shifted through the column in 250 steps to simulate percolation. Each step/shift replaced 1 L of solution which was in contact with 1 kg of solids and hence each step was equal to L/S 1 L/kg. For the sake of simplicity only 1-D transport of eluent (forward flow) was used while neither dispersivity nor dual-porosity were considered.

2.6.2. Initial mineral assemblage

Currently, there is no general approach to specify the exact amount of a particular mineral from the total mass of a specific element determined by sample digestion. In our approach, we assumed that portlandite ($Ca[OH]_2$) will likely determine pH of the system and thus leaching of other elements. Therefore, in the first step, the amount of portlandite in the SD-column was derived to match the decrease in both Ca and alkalinity which was observed between L/S 150 and L/S 175 L/kg (discussed later); 3 mol of portlandite per 1 kg of initial mineral assemblage (mol/kg) were found appropriate. Similarly, the amount of gypsum ($CaSO_4{\cdot}2H_2O$) was adapted to match the decrease in S between L/S 25 and 50 L/kg; this time, about 0.2 mol/kg were found appropriate. These amounts of Ca and S did not account for the entire solid mass; the residual mass was thus distributed between other possible solubility controlling minerals. Of course, amounts of other constituents in these minerals had to be considered as well and the whole procedure was therefore an iteration process. In the end, 3 mol of portlandite, 0.2 mol of gypsum, 2.6 mol of calcite ($CaCO_3$), 0.35

Table 2
Changes to PHREEQC thermodynamic database in addition to those made by Astrup et al. [7]

Phase	Reaction	log k	Refs.
Friedel's salt	$Ca_4Al_2Cl_2(OH)_{12}{\cdot}4H_2O + 12H^+ = 4Ca^{2+} + 2Al^{3+} + 2Cl^- + 16H_2O$	−27.6	[41]
Strätlingite	$Ca_2Al_2(SiO_2)(OH)_{10}{\cdot}3H_2O + 10H^+ = 2Al^{3+} + 2Ca^{2+} + 11H_2O + H_4SiO_4$	49.44	[52]
Ettringite	$Ca_6Al_2(SO_4)_3(OH)_{12}{\cdot}32H_2O + 12H^+ = 6Ca^{2+} + 2Al^{3+} + 3SO_4^{2-} + 44H_2O$	57.45	[53]
Cr-ettringite[a]	$Ca_6Al_2(CrO_4)_3(OH)_{12}{\cdot}26H_2O + 12\ H^+ = 6Ca^{2+} + 2Al^{3+} + 3CrO_4^{2-} + 38H_2O$	60.54	[50]
Monosulphate	$Ca_4Al_2O_6(SO_4){\cdot}6H_2O + 12H^+ = 4Ca^{+2} + 2Al^{+3} + SO_4^{2-} + 12H_2O$	72.57	[53]
Cr-monosulphate[a]	$Ca_4Al_2(CrO_4)(OH)_{12}{\cdot}9H_2O + 12H^+ = 4Ca^{2+} + 2Al^{3+} + CrO_4^{2-} + 21H_2O$	71.62	[54]
Mo-monosulphate[a]	$Ca_4Al_2(MoO_4)(OH)_{12}{\cdot}10H_2O + 12H^+ = 4Ca^{2+} + 2Al^{3+} + MoO_4^{2-} + 22H_2O$	71.66	[55]
Ca-arsenate(I)[a]	$Ca_3(AsO_4)_2{\cdot}3.66H_2O = 3Ca^{2-} + 2AsO_4^{3-} + 3.66H_2O$	−21.0	[56]
Ca-arsenate(II)[a]	$Ca_3(AsO_4)_2{\cdot}4.25H_2O = 3Ca^{2+} + 2AsO_4^{-3} + 4.25H_2O$	−21.0	[56]
Ca-arsenate(III)[a]	$Ca_5(AsO_4)_3OH = 5Ca^{2+} + 3AsO_4^{3-} + OH^-$	−38.04	[56]
Ba-arsenate[a]	$Ba_3(AsO_4)_3 = Ba^{2+} + HAsO_4^{2-}$	−23.53	[57]
Ba-H-arsenate[a]	$BaHAsO_4{\cdot}H_2O = Ba^{2+} + HAsO_4^{2-} + H_2O$	−5.60	[57]
Ca-Sb-OH[a]	$Ca[Sb(OH)_6]_2 = Ca^{2+} + 2Sb(OH)_6^-$	−12.55	[58]

[a] Names used in this study; does not necessarily reflect proper mineral names.

moles of ettringite ($Ca_6Al_2[SO_4]_3[OH]_{12}\cdot 32H_2O$), 0.022 mol of akermanite (Ca_2MgSiO_7), 0.005 moles of barite ($BaSO_4$), and 0.14 mol of zincite (ZnO) formed the mineral assemblage. All these minerals are commonly identified in APC residues [15,22,24]. Compared with the total mass of Ca, S, Al, Si, Ba, and Zn in the SD-residue this accounted for 96% of Ca, 116% of S, 103% of Al, 2% of Si, 110% of Ba, and 101% of Zn respectively. The mineralogy of APC residues is unquestionably much more complicated. However, for a first approximation this assemblage was found to be sufficient.

2.6.3. Determination of sorption sites

As outlined in Section 1 and described in detail in Section 3, the sorption on reactive surfaces is important mechanism controlling leaching from APC residues. In this work we accounted for sorption to hydrous iron (hyd)oxides (HFO) and hydrous aluminium (hydr)oxides (AlO) using the generalized two-layer model of Dzombak and Morel [25]. Amounts of amorphous HFO and amorphous AlO were obtained by independent extractions according to Kostka and Luther [26], and Blakemore et al. [27] respectively. Similarly to Dijkstra et al. [28] we considered HFO and AlO to be equal in the model. Accordingly, the extracted amounts were added up assuming that 1 mol of Fe ~1 mol of Al and recalculated to kg of HFO/kg of solid phase; a gram formula weight of 89 g HFO/mol Fe was used [25]. In the end 6.2 and 5.9 g of HFO/kg of solids were obtained for the FA- and the SD-residue, respectively.

2.6.4. Percolation simulation

During the percolation, portlandite was kept in equilibrium with the solution whereas, in agreement with the speciation calculations performed for the early eluates, both gypsum, calcite and ettringite were kept slightly oversaturated. Furthermore, monosulphate ($Ca_4Al_2O_6[SO_4]\cdot 6H_2O$) and diaspore (AlOOH) which were not considered to be present in the initial assemblage were allowed to precipitate if needed. These phases were suggested by the speciation calculations to be present at later L/S ratios. Monosulphate has recently been reported to form from ettringite at low sulphate concentrations [29]. In the end, developments in pH, alkalinity, and solution concentrations of Ca, S, Al, Si, Ba, and Zn in the SD-column were obtained over the L/S ratio of 250 L/kg.

Sorption to HFO/AlO was tested in preliminary calculations (not shown). Including the previously discussed amounts of reactive surfaces in the preliminary modeling exercise, however, showed minimal influence on leaching of considered elements. Therefore, sorption to HFO/AlO was omitted in the further percolation modeling. Similarly, complexation with DOC was neglected as well as the interaction between DOC and the considered elements were limited.

3. Theory

3.1. Leaching control

As outlined in Section 1, three major groups of elements can be distinguished based on their predominant leaching behavior: availability-controlled elements, solubility-controlled elements, and complexation/sorption-controlled elements.

The availability-controlled elements can basically be seen as readily-soluble compounds. Their release is not limited by solubility constraints as the solution concentrations are well below mineral solubility (e.g. Cl and NaCl). Leaching of readily-soluble compounds is characterized by high initial solution concentrations; i.e. tens to hundreds of grams per liter. Then, rather fast decreases in solution concentrations occur and depletion is assumed [4,20].

Release of solubility-controlled elements is limited by mineral solubility (e.g. Ca and $CaSO_4$). Hence, leaching of the solubility-controlled elements is characterized by relatively stable solution concentrations over long periods of time [30]. Mineral depletion has been suggested by geochemical modeling [31], although not observed in leaching experiments.

Finally, there are sorption/complexation-controlled elements (mostly metals). At the high pH levels observed in leachates from APC residues (pH >11), metal cations (e.g. Pb^{2+}, Ni^{2+}, Cd^{2+}) tend to sorb to reactive surfaces such as HFO/AlO whereas metal oxyanions (e.g. CrO_4^{2-}, MoO_4^{2-}) stay mobile [25,32]. In addition, many metals have high affinity for complexation with DOC and their leaching has been shown to vary proportionally to the amount of DOC [33]. Still, sorption to HFO/AlO or complexation with DOC are not the only processes controlling the leaching of metals. It has been reported that significant amounts of metals (both cations and anions) may be immobilized by substitution in hydrated cement phases such as ettringite [29,34] and thus become rather solubility-controlled.

3.2. L/S ratio

The L/S ratio is defined as volume of a liquid in contact with dry solid material. There are two major applications of L/S ratio within a field of leaching quantification. Firstly, multiplying determined solution concentrations (mg/L) with L/S ratio of an experiment (L/kg) will result in expressing outputs of any leaching scenario as mass released per kilogram of solid phase (mg/kg). This ensures proper comparison of results obtained for the same material in different leaching experiments as well as reciprocal comparison of different leaching scenarios (e.g. landfill versus column). Secondly, assuming knowledge of hydrological conditions in an arbitrary scenario (e.g. landfill) allows us to recalculate any L/S ratio to leaching time. For instance, it takes approximately 100 years to reach L/S ratio of 2 L/kg in a conventional landfill which is roughly 10 m thick, has a dry bulk density of 1.3 kg/dm^3, and the annual precipitation is about 150–250 mm [35].

4. Results and discussion

4.1. General overview

Results of column leaching experiments are discussed in following sections. Fig. 1 shows pH, conductivity, alkalinity, and solution concentrations of readily soluble compounds (i.e. Na, K, and Cl) as functions of the L/S ratio. Solution concentrations of Ca, SO_4^{2-} (shown as S), Al, and Si are shown in Fig. 2. Leaching of Ba, Sr, Cu, Pb, and Zn is shown in Fig. 3 while As, Cr, Sb, V, and Mo are shown in Fig. 4. Leaching of Cd, Fe, Mg, Hg, Mn, Ni, Co, Sn, Ti, and P from both materials was generally found below the associated detection limits (in mg/L): Cd (5×10^{-5}), Fe (2×10^{-2}), Mg (1.4×10^{-1}), Hg (2×10^{-5}), Mn (9×10^{-4}), Ni (6×10^{-4}), Co (2×10^{-4}), Sn (5×10^{-4}), Ti (2×10^{-2}), and P (1×10^{-2}) respectively. These elements are therefore not shown graphically nor discussed. Finally, results for percolation modeling of pH, alkalinity, Ca, S, Al, Si, Ba, and Zn are shown in Fig. 5.

In order to provide a scale for which to relate the leaching data in a long-term perspective, leaching criteria for waste acceptable at landfills for inert-, non-hazardous, and hazardous waste were included in the Figures where appropriate. The limit values are based on leaching from the CEN/TS column test, specifically the concentrations detected in leachates at L/S 0.1 L/kg [6]. In the following text these acceptance criteria are referred to as "limits" unless stated otherwise. An overview of limits for the considered elements can be found in Table 3 together with their associated detection limits.

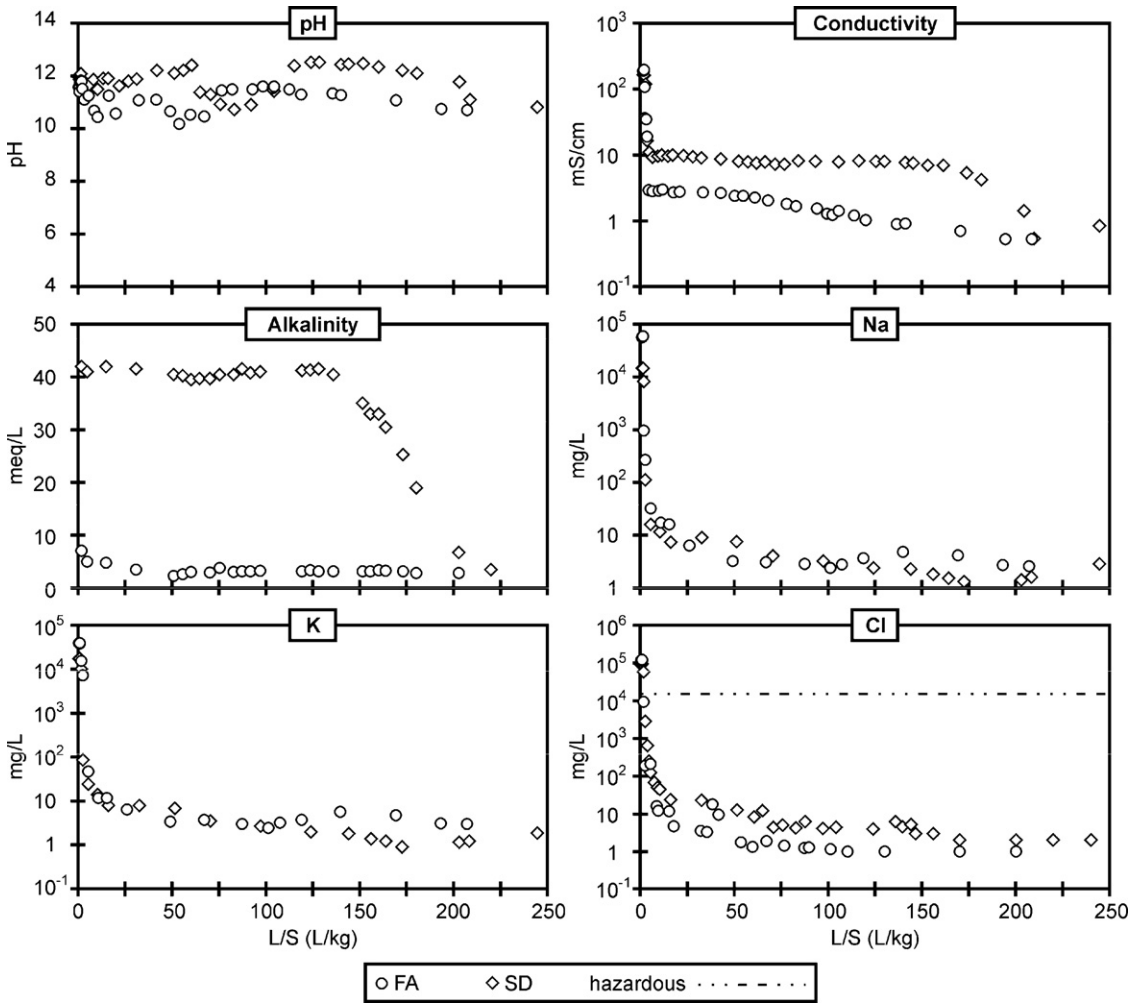

Fig. 1. pH, conductivity, alkalinity and solution concentrations of Na, K, and Cl as function of L/S ratio. Leaching data for FA and SD are represented by open spheres and diamonds, respectively. Leaching criteria for waste acceptable at landfills for hazardous waste is indicated by combined black dashed line if needed.

4.2. pH

Generally, pH in the FA-column was lower than in the SD-column during the course of the experiments except for a period between L/S 70 and 100 L/kg where pH in the SD-column decreased to a minimum of pH 10.7 (Fig. 1).

Table 3
Limit values for waste acceptance at landfills for inert-, non-hazardous-, and hazardous waste [6]. Detection limits (DL) of the used ICP-AES and ion chromatography are shown as well

Element	Inert (mg/L)[a]	Non-hazardous (mg/L)[a]	Hazardous (mg/L)[a]	DL (mg/L)
As	0.06	0.3	3	1×10^{-3}[b]
Ba	4	20	60	1×10^{-3}
Cr (total)	0.1	2.5	15	9×10^{-4}
Cu	0.6	30	60	1×10^{-3}
Mo	0.2	3.5	10	1×10^{-3}
Pb	0.15	3	15	6×10^{-4}
Sb	0.1	0.15	1	1×10^{-4}
Zn	1.2	15	60	4×10^{-3}
Chloride	460	8.5×10^3	15×10^3	1[c]
Sulphate	1.5×10^3	7.0×10^3	17×10^3	0.5[c]

[a] Limit values are based on concentrations obtained at L/S 0.1 L/kg during the CEN/TS column test.
[b] A higher limit of quantification applies to samples with high chloride levels.
[c] Ion chromatography was used.

The somewhat lower pH in the FA-column ($10.2 < pH < 11.8$) could likely be explained by an absence of portlandite which in turn is caused by a significantly lower content of lime (CaO) in the FA-residues; accordingly, during speciation calculations portlandite was found undersaturated in the initial leachates ($SI < -1.3$). Instead, similarly to other studies [7,8,12,29] gypsum, monosulphate, calcite, and ettringite were found either close to equilibrium or oversaturated. Thus, these minerals were assumed to control pH in the FA-column.

Higher pH of the SD-residue ($11.2 < pH < 12.4$) can likely be attributed to the large amounts of unreacted lime added during the flue gas cleaning [1,4]. Consequently, lime dissolves and leachate becomes oversaturated with portlandite which may precipitate. SI of portlandite was SI ~1 in the early eluates from the SD-column; this was consistent with data obtained from pH-dependent leaching experiments on the same material [12]. Dissolution of portlandite explains high pH values which in some cases were close to pH 12.5; i.e. corresponding to a pH of a solution in equilibrium with portlandite. Variations in the pH curve observed in the SD-column between L/S 75 and 125 L/kg corresponded to an apparent depletion of portlandite ($SI < -1$ at L/S 80 L/kg) from the mobile zone that was probably followed by an opening of stagnant zones and subsequent reaction of previously entrapped portlandite with the eluent. Accordingly, late eluates were again found saturated with portlandite (SI ~0.2 at L/S

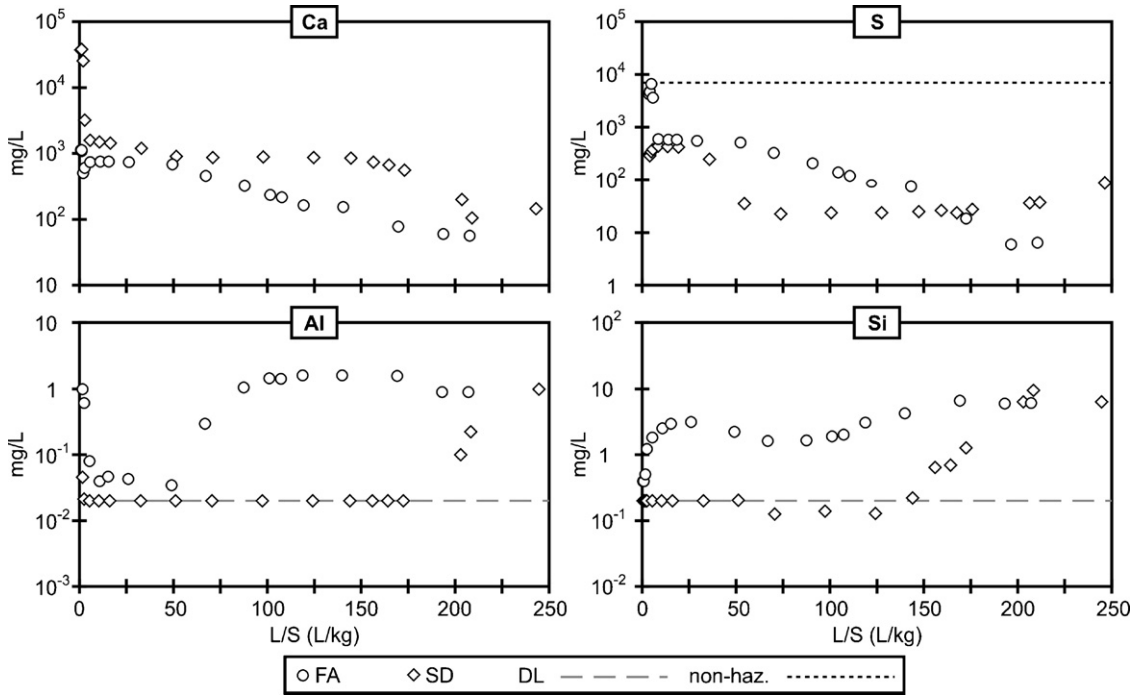

Fig. 2. Solution concentrations of Ca, S, Al, and Si as function of L/S ratio. Leaching data for FA and SD are represented by open spheres and diamonds, respectively. Detection limits (DL) are indicated by grey dashed line where appropriate. Leaching criteria for waste acceptable at landfills for non-hazardous waste (non-haz.) is indicated by black dashed line.

125 L/kg). We believe that equilibrium with soluble phase which was previously depleted may simply be explained by existence of preferential flow patterns and/or dual porosity [36]. Similarly to the FA-column gypsum and calcite were found close to equilibrium or oversaturated. In addition, strätlingite ($Ca_2Al_2[SiO_2][OH]_{10}{\cdot}3H_2O$) was found close to equilibrium in initial leachates.

4.3. Conductivity

Conductivity curves basically reflected leaching of the readily soluble compounds which are discussed later (see Na, K, and Cl). High initial values of 190 mS/cm (FA-column) and 160 mS/cm (SD-column) decreased by more than one order of magnitude within L/S 3 L/kg. Then, stable values were observed, although somewhat higher in the case of the SD-residue. This also corresponded to higher leaching of chloride in the SD-column.

4.4. Alkalinity

Total alkalinity determined in initial leachates was about 6 and 42 meq/L for the FA- and the SD-residue, respectively. Both values were fully comparable with those observed by Astrup et al. [37] for similar types of residues. Alkalinity of leachates from the FA-columns was calculated using a mineral assemblage of gypsum, ettringite and calcite (no portlandite considered); calculated pH and alkalinity were found to 11.04 and 4.7 meq/L, i.e. in fair agreement with the measured values.

As indicated above, portlandite was likely present in the SD-residue and dissolution of portlandite in the SD-column may have caused higher alkalinity. Thus, when portlandite was added to the above mineral assemblage; an alkalinity of 38 meq/L and pH 12.38 were obtained. Again, this is fully comparable with our experimental data. Apparently, dissolution of portlandite caused about seven times higher alkalinity in the leachates from the SD-residue. Hence, depletion of portlandite from the system would eventually lead to a decrease of alkalinity in the SD-column to the level observed in the FA-column since presence of portlandite was the only difference in the considered mineral assemblages. Such a decrease can be seen in the SD-column between L/S 150 and 200 L/kg (Fig. 1).

Today, alkalinity is usually not determined during column percolation experiments. However, as outlined above, alkalinity curve can be used to estimate amount of portlandite in the system which can in turn be used to mimic initial mineral assemblage and further to describe pH development. Therefore, regarding later geochemical modeling, monitoring of alkalinity during percolation experiments should be considered.

4.5. Na, K, and Cl

Leaching curves of Na, K, and Cl from both residues are shown in Fig. 1. Initial release of Na, K, and Cl from the FA-column was about 58×10^3 mg/L, 39×10^3 mg/L and 117×10^3 mg/L respectively. For the SD-column about 14.5×10^3 mg/L, 17.5×10^3 mg/L and 87.5×10^3 mg/L of Na, K, and Cl was measured. The leaching of chloride thereby exceeded limits for hazardous-waste (i.e. 15×10^3 mg/L) by a factor of 6–8 in either material.

In general, high initial leaching of Na, K, and Cl was likely caused by dissolution of the readily soluble salts such as halite (NaCl) and sylvite (KCl). Accordingly, concentrations of Na, K, and Cl in the FA-column showed an excellent fit when compared on a mole-to-mole basis. The quotient of the sum of Na^+ and K^+ (mol/L) to Cl^- (mol/L) was close to 1 during the initial leaching, i.e. between L/S 0 and L/S 5 L/kg. In the SD-column such "balance" resulted in a large fraction of "free" Cl^-. In other words there was not enough Na^+ and K^+ to match Cl^-. As discussed above, the SD-residue contains large amounts of lime which dissolves rapidly. Hence, "free" Ca^{+2} and Cl^- may form hydrophilite ($CaCl_2$) which dissolves immediately; hydrophilite was determined experimentally in untreated APC residues [20,38]. Indeed, when halite, sylvite, and hydrophilite

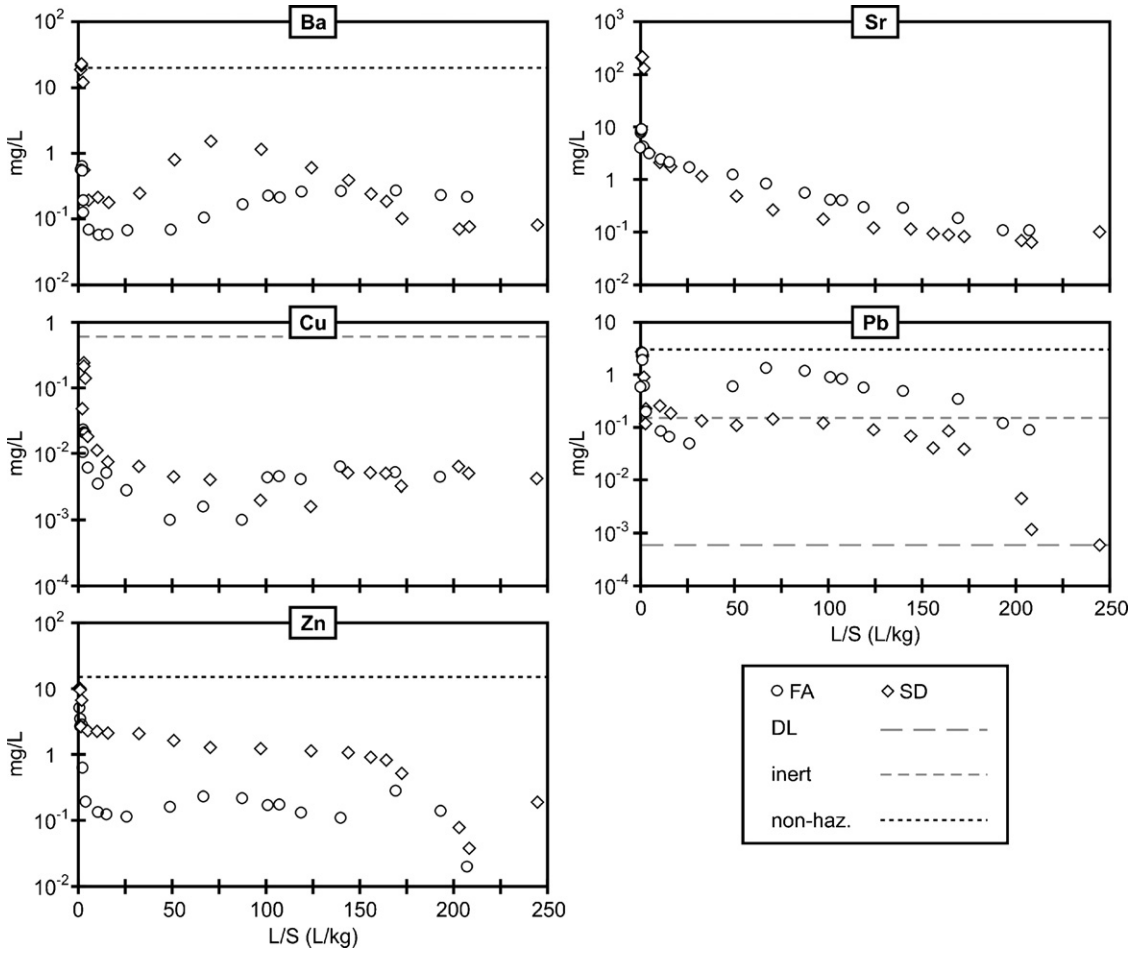

Fig. 3. Solution concentrations of Ba, Sr, Cu, Pb, and Zn as function of L/S ratio. Leaching data for FA and SD are represented by open spheres and diamonds, respectively. Detection limits (DL) are indicated by wide grey dashed line where appropriate. Leaching criteria for waste acceptable at landfills for inert and non-hazardous waste are indicated by short grey dashed line and black dashed line (non-hazardous), respectively.

were considered to dissolve simultaneously an excellent mole-to mole fit was obtained. Similarly to the FA-column this happened within L/S 5 L/kg.

Interestingly, solution concentrations of Na, K, and Cl were found constant in the first three samples from both columns; i.e. at L/S 0.1, 0.2, and 0.5 L/kg. This would suggest solubility control to take place despite both halite and sylvite being calculated to be undersaturated ($-1.5 < SI < -0.5$). As discussed previously, those saturation indices were calculated using the Davies equation and since the activity coefficients of Na^+, K^+, and Cl^- are known to increase rapidly at $I > 0.7$ [39] the actual solubility of these phases decreases. Lower solubility would consequently cause an apparent undersaturation of these minerals in our system.

Overall, typical availability-control leaching behavior was observed for Na, K, and Cl in both columns during the initial L/S 10 L/kg. A slight "tailing" of Cl appeared in both columns; i.e., the solution concentrations decreased slowly after L/S 5 L/kg even though dissolution of Cl-containing compounds was not expected to be limited by solubility constrains. Tailing could be attributed to an existence of mobile and stagnant zones and slow diffusion-controlled transfer of mass between these zones; as mentioned in the pH discussion. Another reason for lower mobility of chloride could be precipitation of Friedel's salt ($Ca_4Al_2Cl_2[OH]_{12}{\cdot}4H_2O$) which often forms in cementious systems [40,41]. In either case, only about a half of the total chloride was removed during the course of our experiments as indicated in Table 4.

4.6. Calcium (Ca) and sulphate (SO_4^{2-})

Concentrations of Ca in leachates from the FA-residue were found relatively stable between 0.8×10^3 and 1.0×10^3 mg/L within the initial L/S 50 L/kg (Fig. 2). Then, a slow decrease towards high L/S could be observed. The shape of the leaching curve was similar to that of SO_4^{2-} (SO_4^{2-} is shown as S) indicating that both elements could be controlled by the same mineral (e.g. gypsum). The leaching of SO_4^{2-} from the FA-columns was between 4.2×10^3 and 6.7×10^3 mg/L at L/S < 2 L/kg; i.e. almost level with the limits

Table 4
Fractions of different elements (% of their initial mass) leached during the course of the column experiments (i.e. L/S 207 L/kg for the FA-residue and L/S 245 L/kg for the SD-residue) as calculated by cumulative Simpson's integration with uneven spacing [18]

Element	Removed mass	FA	SD	Element	Removed mass	FA	SD
Na	%	~65	~103	Sr	%	~41	~71
K	%	~82	~115	Cr	%	<1	<1
Cl	%	~53	~64	Mo	%	~34	~38
Ca	%	~39	~68	Sb	%	~1	<1
S	%	~104	~59	Cu	%	<1	<1
Si	%	< 1	< 1	Cd	%	<1	<1
Al	%	< 1	< 1	Pb	%	~1.6	~1.1
As	%	< 1	< 1	Zn	%	< 1	~3
Ba	%	~3.5	~24	V	%	~4.4	~3.7

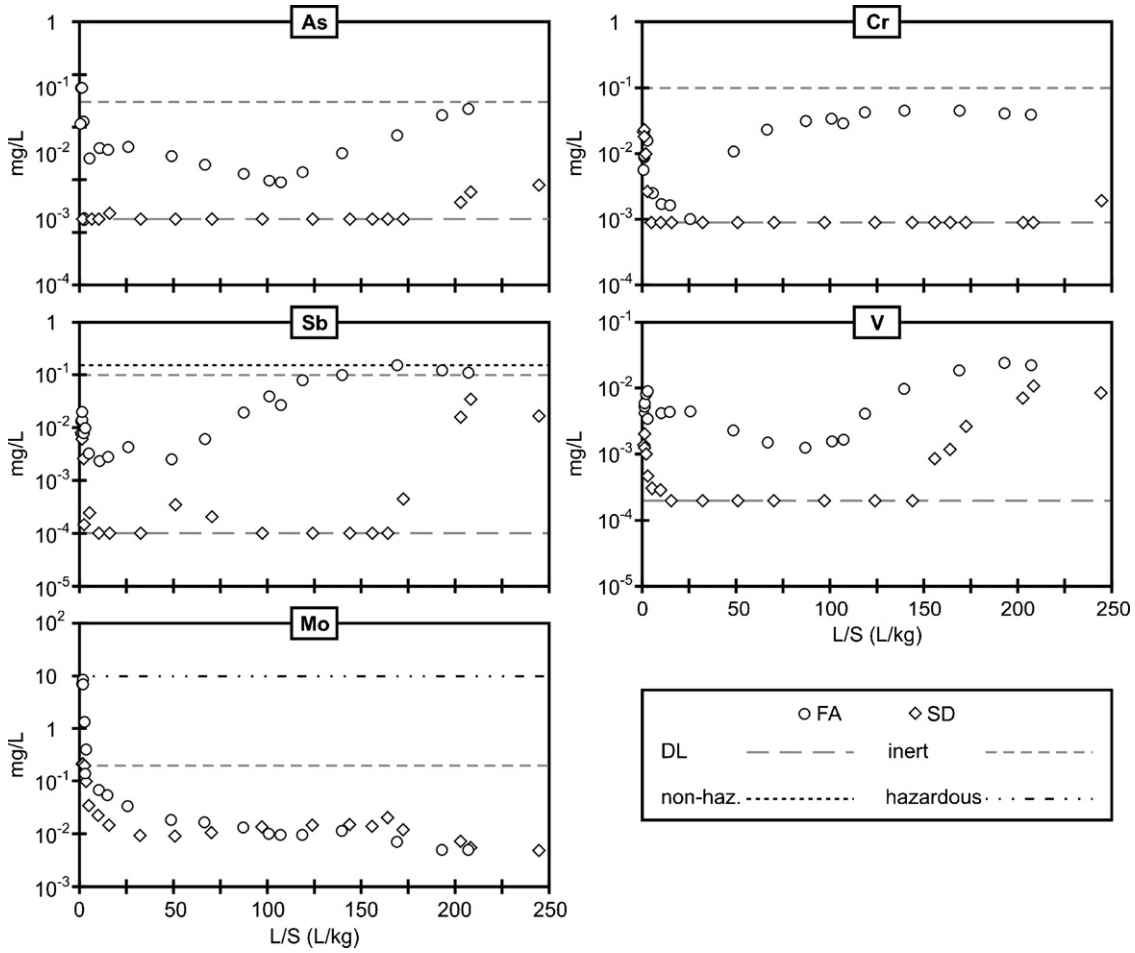

Fig. 4. Solution concentrations of As, Cr, Sb, V, and Mo as function of L/S ratio. Leaching data for FA and SD are represented by open spheres and diamonds, respectively. Detection limits (DL) are indicated by wide grey dashed line where appropriate. Leaching criteria for waste acceptable at landfills for inert, non-hazardous, and hazardous waste are indicated by grey dashed-, black dashed (non-hazardous), and combined black dashed line, respectively.

for non-hazardous waste. Such high concentrations could not be explained by dissolution/precipitation of common S-containing minerals like gypsum or anhydrite ($CaSO_4$) as the Ca-S molar ratio was found to 5:1. Between L/S 2 and 150 L/kg, solution concentrations of Ca and SO_4^{2-} from the FA-column showed an excellent fit on a mole-to-mole basis (not shown) and thus gypsum (SI ~0.1) was considered to govern release of both Ca and SO_4^{2-}. After L/S 150 L/kg gypsum is likely being depleted (SI < −1).

As indicated previously, high initial concentrations of Ca (~37×10^3 mg/L) in the SD-column were probably caused by dissolution of the excess lime injected in the flue-gas-cleaning system. In addition, based on the speciation calculations portlandite (SI ~1) and gypsum (SI ~0.1) were suggested to control leaching of Ca and SO_4^{2-} from the SD-column. More specifically, Ca concentrations between L/S 5 and 150 L/kg were in good agreement with calculated equilibrium with portlandite which varied somewhat within this L/S range. Local "depletion" of portlandite (SI < −1) likely caused the aforementioned pH decrease between L/S 70 and 100 L/kg (see Section 4.2). In addition, slight changes in alkalinity can be observed as well. After L/S 100 L/kg, portlandite was again in equilibrium with the solution (SI >0) and consequently an increase in pH could be observed after L/S 100 L/kg in the SD-column. As outlined previously, this behavior is believed to be caused by depletion of portlandite from the mobile zone and later opening of new mobile zone due to removal of mass from the column. After L/S 150 L/kg, a second "depletion" of portlandite took place. This time, a significant drop in alkalinity to the level of the FA-residue (no portlandite) could be observed; moreover, pH decreased as well. The leaching of SO_4^{2-} corresponded to equilibrium with gypsum up to L/S 50 L/kg. After L/S 50 L/kg, a one order of magnitude decrease in sulphate concentrations could be observed; concentrations corresponded to equilibrium with ettringite. Hence, a lack of gypsum combined with solubility control via a less soluble mineral (e.g. ettringite) could explain the observed leaching behavior. Ettringite was also suggested to be the controlling mineral in pH-static leaching experiments performed on same material [12]. After L/S 150 L/kg an increase in SO_4^{2-} could be observed simultaneously with a Ca decrease (depletion of portlandite). This indicates an enhanced dissolution of ettringite because of lack of Ca.

Compared to the initial amount in the solid phase (Table 1) about 39% and 68% of Ca was calculated to be removed from the FA- and the SD-residue respectively (Table 4). Similarly, approximately 104% and 59% of S were calculated to be removed from the FA- and the SD-residue. Although more than three orders of magnitude decreases in SO_4^{2-} solution concentrations were observed during the experimental period, total depletion of SO_4^{2-} from the FA-column seems unlikely. Standard analytical uncertainties should naturally be considered, and the removed fractions (Table 4) should be seen more as indicators of possible depletion rather than exact values.

4.7. Aluminum (Al) and Silicium (Si)

As can be seen in Fig. 2 the initial concentrations of Al in the FA-column decreased by one order of magnitude to 5×10^{-2} mg/L and stayed at this level until L/S 50 L/kg after which a 20-fold increase in solution concentrations occurred; stable concentrations about 1 mg/L were observed between L/S 75 and 200 L/kg. In contrast, concentrations of Al in leachates from the SD-column remained below the detection limit of 2×10^{-2} mg/L until L/S 175 L/kg. At this point, an increase to the level observed for the FA-residue occurred. From the speciation calculations, dissolution of ettringite was suggested to cause the observed behavior. Further, stable solution concentrations after L/S 50 L/kg (FA-column) and L/S 175 L/kg (SD-column) suggested solubility control; leachates from both columns were found in equilibrium with diaspore. Hence, precipitation of diaspore could explain the observed concentration plateau.

The leaching of Si showed patterns similar to those of Al: i.e. stable and detectable concentrations (~5 mg/L) in leachates from the FA-residue whereas leachates from the SD-column were below the detection limit of 0.2 mg/L until L/S 150 L/kg. Again, a late increase in leaching from the SD-residue matched the concentrations observed in case of the FA-column, i.e. around 6 mg/L. Dissolution of akermanite or strätlingite caused by a depletion of other Ca-containing minerals is believed to explain this behavior. Both minerals were also suggested to control the Si leaching from bottom ashes and APC residues [12,42].

Overall, an increase in solution concentrations of both Al and Si was observed in the late stage of the leaching sequence in both columns. This increase appeared to be related with a decrease in Ca concentrations; most pronounced in the SD-column (Fig. 2). Thus, leaching of Al can be linked to dissolution of ettringite due to depletion of Ca in the portlandite–gypsum system. This dissolution is followed by precipitation of diaspore which would control the Al solution concentrations around 1 mg/L. Overall, throughout the entire 2 years leaching period, less than 1% of the initial amount of Si and Al has leached from either column (Table 4).

4.8. Barium (Ba) and Strontium (Sr)

Leaching of Ba from both residues had a similar pattern except concentrations were more than one order of magnitude higher in case of the SD-residue: i.e. 0.8 mg/L in the FA- and 20 mg/L in the SD-column, respectively (Fig. 3). Notably, the latter reached the upper limits for non-hazardous waste (Table 3). In either case, high initial concentrations were followed by a decrease within L/S 25 L/kg after which an increase occurred again; this being more pronounced in the SD-column. There appeared to be a relation between leaching of Ba and S; and again this was more pronounced in the SD-column. It can be seen that the drop in S concentrations at L/S 50 L/kg resulted in an increase in Ba concentrations. Vice versa, a slow increase in S concentrations at late L/S ratios (dissolution of ettringite) caused decrease in Ba concentrations again. Barite, $Ba(Ca)SO_4$ solid solution, $Ba(S,Cr)O_4$ solid solution, and $Ba(Sr)SO_4$ solid solution [43–45] were suggested from the speciation calculations to control the solution concentrations. Accordingly, an interaction between gypsum, ettringite, and barite could be a likely explanation of S, Al, and Ba leaching.

Similarly to Ba the leaching patterns of Sr were almost identical in both columns (Fig. 3). Yet again, Sr solution concentrations in the early eluates from the SD-column were twenty-fold of those in the FA-column: i.e. 210 mg/L and 9 mg/L, respectively. The only mineral found in our database that could explain Sr concentrations above 100 mg/L was SrF_2. Despite the initial difference both leaching curves reached the same level (5 ± 2 mg/L) at L/S 2 L/kg. From that point on, both curves slowly decreased with increasing L/S ratio. Finally after L/S 200 L/kg, concentrations about 0.1 mg/L were detected. The resemblance between both curves suggested identical controlling processes after L/S 2 L/kg. As mentioned in the Ba discussion, $Ba(Sr)SO_4$ solid solution was found within the SI boundaries; moreover, its solubility was close to the Sr concentrations observed at L/S 2 L/kg. Accordingly, slow depletion of $Ba(Sr)SO_4$ solid solution from the mobile zone is suggested to cause the presented leaching of Sr after L/S 2 L/kg.

Overall, during the course of the experiments about 3.5% and 41% of initially present Ba and Sr was released from the FA-residues. In accordance with the higher initial concentrations of both elements in leachates from the SD-column the total released mass of Ba and Sr was significantly higher in case of the SD-residues; i.e. 24% and 71%, respectively (Table 4). In both cases these high values are comparable with the leaching of Ba and Sr in batch pH-static experiments [12]. Apparently, a significant fraction of particularly Sr is "available" at natural pH of both residues; at pH >11.

4.9. Copper (Cu)

Initial solution concentrations of Cu were about 0.02 mg/L and 0.2 mg/L in the FA- and the SD-residue, respectively (Fig. 3); i.e. within the limits for inert waste. Initial Cu leaching resembled the wash-out of DOC (not shown graphically) which is commonly suggested to be the major process controlling Cu via complexation [12,46–48]. DOC in eluates from the FA-column decreased from 6 to 1 mg/L within L/S 10 L/kg. Analogically, DOC in the SD-column decreased from 41 to 3 mgl/L within the same L/S range. Similarly for both materials, leaching of Cu decreased rapidly during the initial leaching period and stayed around 1–6 μg/L for the rest of the experiments. This level could also be explained by solubility of $Cu(OH)_2(s)$ which has been suggested to control the leaching of Cu from APC residues at pH >10 [12]. In total, less than 1% of Cu was leached from either residue (Table 4).

4.10. Lead (Pb)

Release of Pb from both residues was identical up to L/S 30 L/kg (Fig. 3). Limits for non-hazardous waste were nearly exceeded as the solution concentrations were found close to 3 mg/L. High leaching of Pb at high levels of salts pointed to inorganic complexation [1,12]; in addition, sorption to HFO/AlO can be used to explain the leaching of Pb [8]. Between L/S 5 and 50 L/kg, the leaching of Pb from both FA- and SD-residue decreased below the limits for inert waste. At L/S 50 L/kg a one order of magnitude increase in Pb concentrations could be observed in the FA-column. This corresponded with the previously mentioned behavior of Ca, S, and Al (i.e. ettringite dissolution). Gougar et al. [29] reported incorporation of Pb^{2+} in the ettringite structure. Hence, a mobilization of Pb due to dissolution of its bearing phase appeared to be a plausible explanation since desorption of Pb^{2+} from HFO/AlO surfaces is not expected at pH >10 [32]. Only a little increase in the leaching of Pb could be observed in the SD-column. In addition, Al concentrations were found below the detection limit. Thus, both substitution to ettringite and sorption to HFO/AlO could be the controlling processes. The final leached amounts corresponded to 110 mg/kg for the FA- and 22 mg/kg for the SD-residue, respectively. This was approximately 1.6% and 1.1% of the total mass of Pb in solid phase.

4.11. Zinc (Zn)

Initial leaching of Zn from both materials was rather alike (Fig. 3) and solution concentrations between 5 and 10 mg/L classified both residues acceptable to landfills for non-hazardous waste. After L/S 5 L/kg, concentrations leveled at 0.2 and 1 mg/L in FA-

and SD-column, respectively. In accordance with recent studies, zincite and also willemite (Zn_2SiO_4) were suggested to possibly control the solution concentrations [7,12]. A concentration decrease observed after L/S 170 L/kg in both residues could be caused by two different mechanisms. Firstly, it could be linked with changes in pH between L/S 125 and 250 L/kg (see Fig. 1). Solubility of zincite is 2.85×10^{-2} mmol/L (or 1.8 mg/L) at pH 12.4 and about 3.71×10^{-3} mmol/L (or 0.25 mg/L) at pH 11.5. Secondly, as the effect of pH was not clearly pronounced in the FA-column, the late decrease in Zn concentrations may also indicate practical depletion of available Zn. The total leached amount corresponded to only 1% and <3% for the FA- and the SD-residue, respectively.

4.12. Leaching of oxyanions

At high pH and oxidizing conditions arsenic (As), chromium (Cr), antimony (Sb), vanadium (V), and molybdenum (Mo) are likely to form oxyanions: AsO_4^{3-}, CrO_4^{2-}, $Sb(OH_6)^-$, VO_4^{3-}, and MoO_4^{2-} [32,39]. As such, they become rather mobile since sorption to HFO/AlO can be excluded. In addition, no "simple" solubility controlling minerals are generally suitable to explain the observed solution concentrations [42]. In this study, the leaching behavior of As, Cr, Sb, and V was significantly different between the two materials; consequently these elements are discussed separately for each residue. The release of Mo showed no difference between the two columns and is therefore discussed together for both residues.

4.12.1. Leaching of As, Cr, Sb, and V from the FA-residue

Concentrations of As, Cr, Sb, and V in leachates from the FA-residue were, contrary to the SD-residue, above their detection limits in all analyzed samples (Fig. 4). The initial leaching period was characterized by decreases in Cr and Sb concentrations, while V was increasing until L/S 2 L/kg and then decreasing afterwards. The concentrations in all samples were below limits for inert waste. Above L/S 50–100 L/kg, an increase in solution concentrations of all four elements was observed. In case of Cr and Sb this increase corresponded well with Al release. Late leaching of oxyanions has been suggested [49], however linked with significant changes in pH which was not the case in our experiments. Cr, Sb and V appeared to reach a concentration plateau at L/S >125 L/kg whereas this was not observed for As. Notably, solution concentrations of Cr, Sb, and V *exceeded* the values observed during the initial leaching period as well as limits for non-hazardous waste in the case of Sb. Today, no limits are set for V. However, release profile presented here suggests that the long-term leaching of V may be of importance.

Based on the speciation calculations two possible minerals were suggested to control Cr release: Cr-containing analogue of ettringite ($Ca_6Al_2[CrO_4]_3[OH]_{12}\cdot 26H_2O$) and $Ba(S,Cr)O_4$ solid solution [44,50]. The solubility of the latter phase could explain the level observed between L/S 100 and 200 L/kg. For Sb, no suitable mineral was found within the SI range of $-1 < SI < 1$ as all Sb-containing minerals were found undersaturated by several orders of magnitude. Release curves of As and V were found slowly decreasing towards L/S 100 L/kg where an increase in the leaching was observed again. In accordance with Saikia et al. [34], $Ca_3(AsO_4)_2$ and $Ca_3(VO_4)_2$ were found within the considered SI interval.

As mentioned previously, ettringite was suggested to form in the leaching system. This mineral could affect the release of the abovementioned oxyanions by substitution of anions (e.g. AsO_4^{3-}, CrO_4^{2-}, $Sb[OH_6]^-$, and VO_4^{3-}) in its structure [29,34]. Thus assuming substitution, precipitation of ettringite would result in incorporation of oxyanions hence lower their solution concentrations; vice versa, ettringite dissolution enhanced by the exhaustion of major elements would lead to increased solution concentrations of the substituting oxyanions, as these would stay in solutions as "free" ions at high pH levels observed in these systems.

4.12.2. Leaching of As, Cr, Sb, and V from the SD-residue

It could be seen in Fig. 4 that in case of the SD-residue the initial solution concentrations of As, Cr, Sb, and V decreased rapidly within L/S 5 L/kg. Between L/S 10 and 150 L/kg solution concentrations of all four elements were found below their detection limits (shown in Table 3). However, at L/S 150 L/kg an increase in the leaching of Sb and V was detected; somewhat lower concentration levels than in the FA-column were reached. Arsenic concentrations increased as well, although not as dramatically and also at somewhat higher L/S ratio of 175 L/kg. The leaching of Cr did not appear to be affected at all and its solution concentrations were found close to the detection limit.

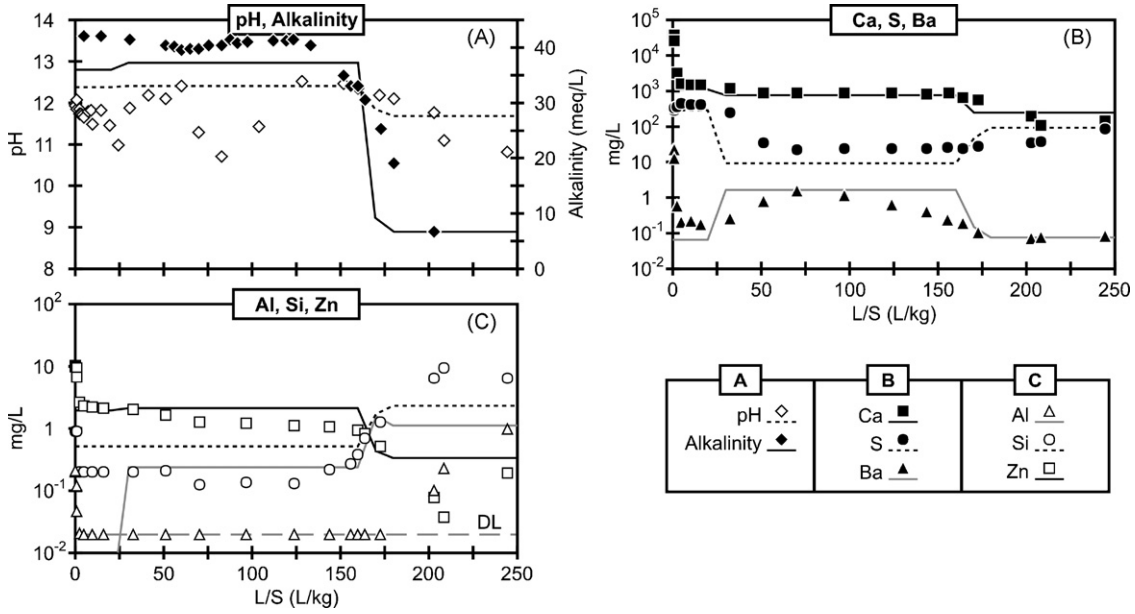

Fig. 5. Results of forward percolation modeling compared with experimental data for the SD column. Experimental data in figure (A), (B), and (C) are represented by points while model predictions are expressed in form of associated lines (see legend). Grey dashed line in figure (C) (not shown in legend) refers to a detection limit (DL) of Al.

4.12.3. Molybdenum (Mo)

Leaching curve of Mo was identical for both materials; solution concentrations decreased during the initial period and then leveled at 1×10^{-2} mg/L. The initial release of Mo from the FA-residue leveled with the limits for hazardous waste whereas the SD-residue could be considered inert waste (Fig. 4). Unlike other oxyanions, MoO_4^{2-} is not linked with the precipitation/dissolution of ettringite as it has been shown unfavorable for substitution due to a difference in size compared with SO_4^{2-} [51]. In accordance with previous studies [12,33], powellite ($CaMoO_4$) was shown plausible to explain the high initial concentrations in the FA-residue (i.e. around 10 mg/L). Complexation with the fulvic part of DOC and/or complexation on HFO/AlO has recently been suggested as possible controlling processes for Mo [47]; Mo release curves in these experiments were in fact comparable with the curves for Cu (Fig. 3).

4.13. Results of percolation modeling for the SD-column

An adequate fit between modeled and measured data was obtained for pH and alkalinity (Fig. 5); the observed decreases are predicted in both cases. Further, excellent model predictions were obtained for Ca, S, Ba and Zn while the leaching of Al and Si was predicted generally well, i.e. within one order of a magnitude.

These predictions were accomplished using a rather "simple" set of minerals; the modeled L/S ratio would correspond to over 10,000 years in typical landfill. For the sake of simplicity, only the solubility-controlled elements were considered thus both DOC complexation and sorption to HFO/AlO could be omitted. Moreover, percolation was set-up using default parameters in PHREEQC (i.e. assuming equilibrium) and no parameter fitting was used. As calculated from the leaching curves, between 20% and 40% of initially present mass was removed within L/S 2 L/kg, primarily due to removal of readily soluble salts. Such removal of solids will influence flow conditions in the column because of dynamic changes in porosity. This issue was not considered in our modeling exercise.

Nevertheless, in spite of being a simplified system, the modeling provided useful insight. Overall, the interaction between portlandite, gypsum and ettringite was shown crucial as these minerals influenced both pH and leaching of major elements (i.e. Ca and S), which in turn had an impact on the remaining elements. Calcite played limited role at pH >10.5 in the portlandite–gypsum–ettringite governed system. Similarly, the initial pH of the eluent (i.e. pH of distilled water before entering the columns) had only negligible effect (modeled, not shown) due to the huge acid-neutralization capacity of the residues [37].

5. Conclusions

Leaching from two different APC residues was monitored during 24 months of laboratory percolation experiments. Standard-based column test was extended up to L/S 250 L/kg (i.e. >10,000 years in a typical landfill). In addition, the leaching data was subjected to a two-step geochemical modeling approach. At first, possible solubility-controlling minerals were identified. Next, a hypothetical mineral assemblage was defined to comply with total composition data, and the leaching of Ca, S, Al, Si, Ba, and Zn was modeled in simplified percolation scenario. Based on the mineral assemblage the pH and alkalinity was also modeled. Finally, the removal of elements was calculated from the leaching curves by numerical integration. Specific conclusions are:

- pH did not change dramatically during the entire leaching period and was controlled by dissolution/precipitation of (i) the gypsum-ettringite system (FA-residue) and (ii) the portlandite–gypsum–ettringite system (SD-residue)
- Leaching of Ca, S, Al, Si, Ba, and Zn was controlled by dissolution/precipitation of the following minerals: portlandite, gypsum, ettringite, diaspore, akermanite, monosulphate, strätlingite, barite and zincite. These minerals were suggested by speciation calculations and further confirmed by forward geochemical modeling of the release from the SD-column over L/S 250 L/kg
- Depletion of some of the above considered minerals may enhance dissolution of the other minerals which in turn results in increased leaching of many elements. An example of such behavior could be increased leaching of oxyanions (especially Sb and Cr) at high L/S ratios possibly due to dissolution of ettringite-like phases
- Substantial amounts of Na, K, Cl, Ca, S, Ba, Sr, and Mo were calculated to be removed based on the observed leaching data
- The leaching of Cd, Fe, Mg, Hg, Mn, Ni, Co, Sn, Ti, and P was mostly found below detection limits of used ICP-AES analysis
- About 97–99% of the total content of metals (i.e. As, Cu, Cd, Pb, Zn, Cr, and Sb) remained in the solid material after 2 years of column leaching, corresponding to more than 10,000 years in typical landfill

Finally, according to European environmental policy both residues are classified as hazardous waste based on their composition. However, according to the leaching-based classification only a few parameters exceeded the limits for non-hazardous landfills. The major problem was high leaching of salts (chloride and sulphate); in addition, few metals (e.g. Pb and Ba) were found close to the upper limits for non-hazardous waste. An easy technical solution could be a simple pre-washing of the residues. A significant fraction of Na, K, and Cl will obviously be removed while Pb can be removed as well; a rather significant fraction of Pb was shown to be easily removable during wash-out of salts likely due to inorganic complexation [1,12]. As for Ba, it is probable that some fraction of Ba will be removed together with sulphate. Hence, the pre-washing step may eventually result in changing the category to "non-hazardous". Overall, it is clear that environmental impacts from leaching should not be related to total composition of the residues.

Acknowledgments

This research was jointly supported by I/S Amagerforbrænding, I/S Vestforbrænding, Aarhus Kommunale Værker, and DONG Energy A/S. The viewpoints presented in this study are solely the responsibility of authors.

References

[1] A.J. Chandler, T.T. Eighmy, J. Hartlem, O. Hjelmar, D.S. Kosson, S.E. Sawell, H.A. van der Sloot, J. Verlow, Municipal Solid Waste Incinerator Residues, Elsevier Science, Amsterdam, 1997.
[2] Miljøstyrelsen (Ministry of Environment), Affaldsstatistik 2004: Orientering fra Miljøstyrelsen Nr. 7, 2005.
[3] Council Directive 91/689/EEC of 12 December 1991 on hazardous waste, European Union, Brussels, 1991.
[4] O. Hjelmar, Disposal strategies for municipal solid waste incineration residues, Journal of Hazardous Materials 47 (1–3) (1996) 345–368.
[5] Council Directive 99/31/EC of 26 April 1999 on the landfill of waste, European Union, Brussels, 1999.
[6] Council Decision of 19 December 2002 establishing criteria and procedures for acceptance of waste at landfills pursuant to Article 16 and Annex II to Directive 1999/31/EC, European Union, Brussels, 2002.
[7] T. Astrup, J.J. Dijkstra, R.N.J. Comans, H.A. van der Sloot, T.H. Christensen, Geochemical modeling of leaching from MSWI air-pollution-control residues, Environmental Science & Technology 40 (11) (2006) 3551–3557.
[8] J.J. Dijkstra, Development of a consistent geochemical modelling approach for leaching and reactive transport processes in contaminated materials [Ph.D. thesis], Wageningen University, The Netherlands, 2007.

[9] H.A. van der Sloot, J.C.L. Meeussen, A. Van Zomeren, D.S. Kosson, Developments in the characterisation of waste materials for environmental impact assessment purposes, Journal of Geochemical Exploration 88 (1–3) (2006) 72–76.
[10] J.A. Meima, R.N.J. Comans, Geochemical modeling of weathering reactions in municipal solid waste incinerator bottom ash, Environmental Science & Technology 31 (5) (1997) 1269–1276.
[11] J.A. Meima, R.N.J. Comans, Application of surface complexation precipitation modeling to contaminant leaching from weathered municipal solid waste incinerator bottom ash, Environmental Science & Technology 32 (5) (1998) 688–693.
[12] J. Hyks, T. Astrup, T.H. Christensen, Influence of test conditions on solubility controlled leaching predictions from air-pollution-control residues, Waste Management & Research 25 (5) (2007) 457–466.
[13] O. Hjelmar, J. Holm, K. Crillesen, Utilisation of MSWI bottom ash as sub-base in road construction: first results from a large-scale test site, Journal of Hazardous Materials 139 (3) (2007) 471–480.
[14] P. Fermo, F. Cariati, A. Pozzi, F. Demartin, M. Tettamanti, E. Collina, M. Lasagni, D. Pitea, O. Puglisi, U. Russo, The analytical characterization of municipal solid waste incinerator fly ash: methods and preliminary results, Fresenius Journal of Analytical Chemistry 365 (8) (1999) 666–673.
[15] P. Fermo, F. Cariati, A. Pozzi, M. Tettamanti, E. Collina, D. Pitea, Analytical characterization of municipal solid waste incinerator fly ash Part II, Fresenius Journal of Analytical Chemistry 366 (3) (2000) 267–272.
[16] C.A. Johnson, M. Kaeppeli, S. Brandenberger, A. Ulrich, W. Baumann, Hydrological and geochemical factors affecting leachate composition in municipal solid waste incinerator bottom ash Part II. The geochemistry of leachate from Landfill Lostorf, Switzerland, Journal of Contaminant Hydrology 40 (3) (1999) 239–259.
[17] CEN, Characterisation of waste – leaching behaviour tests – Up-flow percolation test (under specified conditions), CEN/TS 14405, 2004.
[18] D.C. Hanselman, B.L. Littlefield, Mastering Matlab 7, Prentice Hall, USA, 2004.
[19] D.L. Parkhurst, C.A.J. Appelo, User's guide to PHREEQC (Version 2) – a computer program for speciation, batch-reaction, one-dimensional transport, and inverse geochemical calculations, U.S. Geological Survey Water-Resources Investigations Report 99-4259, 1999.
[20] T.T. Eighmy, J.D. Eusden, J.E. Krzanowski, D.S. Domingo, D. Stampfli, J.R. Martin, P.M. Erickson, Comprehensive approach toward understanding element speciation and leaching behavior in municipal solid-waste incineration electrostatic precipitator ash, Environmental Science & Technology 29 (3) (1995) 629–646.
[21] C.S. Kirby, J.D. Rimstidt, Mineralogy and surface-properties of municipal solid-waste ash, Environmental Science & Technology 27 (4) (1993) 652–660.
[22] L. Le Forestier, G. Libourel, Characterization of flue gas residues from municipal solid waste combustors, Environmental Science & Technology 32 (15) (1998) 2250–2256.
[23] F.Y. Chang, M.Y. Wey, Comparison of the characteristics of bottom and fly ashes generated from various incineration processes, Journal of Hazardous Materials 138 (3) (2006) 594–603.
[24] M. Li, J. Xiang, S. Hu, L.S. Sun, S. Su, P.S. Li, X.X. Sun, Characterization of solid residues from municipal solid waste incinerator, Fuel 83 (10) (2004) 1397–1405.
[25] D.A. Dzombak, F.M.M. Morel, Surface Complexation Modeling: Hydrous Ferric Oxides, John Wiley & Sons, Inc., New York, 1990.
[26] J.E. Kostka, G.W. Luther, Partitioning and speciation of solid-phase iron in salt-marsh sediments, Geochimica et Cosmochimica Acta 58 (7) (1994) 1701–1710.
[27] L.C. Blakemore, P.L. Searle, B.K. Daly, Methods for chemical analysis of soils, Science Report 80, NZ Soil Bureau: Lower Hutt, New Zealand, 1987.
[28] J.J. Dijkstra, J.C.L. Meeussen, R.N.J. Comans, Leaching of heavy metals from contaminated soils: an experimental and modeling study, Environmental Science & Technology 38 (16) (2004) 4390–4395.
[29] M.L.D. Gougar, B.E. Scheetz, D.M. Roy, Ettringite and C-S-H Portland cement phases for waste ion immobilization: a review, Waste Management 16 (4) (1996) 295–303.
[30] D.S. Kosson, H.A. vanderSloot, T.T. Eighmy, An approach for estimation of contaminant release during utilization and disposal of municipal waste combustion residues, Journal of Hazardous Materials 47 (1–3) (1996) 43–75.
[31] T. Astrup, H. Mosbaek, T.H. Christensen, Assessment of long-term leaching from waste incineration air-pollution-control residues, Waste Management 26 (8) (2006) 803–814.
[32] W. Stumm, J.J. Morgan, Aquatic Chemistry, 3rd ed., John Wiley & Sons, Inc., New York, 1996.
[33] C.A. Johnson, M. Kersten, F. Ziegler, H.C. Moor, Leaching behaviour and solubility – controlling solid phases of heavy metals in municipal solid waste incinerator ash, Waste Management 16 (1–3) (1996) 129–134.
[34] N. Saikia, S. Kato, T. Kojima, Behavior of B, Cr, Se, As, Pb, Cd, and Mo present in waste leachates generated from combustion residues during the formation of ettringite, Environmental Toxicology and Chemistry 25 (7) (2006) 1710–1719.
[35] O. Hjelmar, Leachate from land disposal of coal fly-ash, Waste Management & Research 8 (6) (1990) 429–449.
[36] M.L. Brusseau, Q.H. Hu, R. Srivastava, Using flow interruption to identify factors causing nonideal contaminant transport, Journal of Contaminant Hydrology 24 (3–4) (1997) 205–219.
[37] T. Astrup, R. Jakobsen, T.H. Christensen, J.B. Hansen, O. Hjelmar, Assessment of long-term pH developments in leachate from waste incineration residues, Waste Management & Research 24 (5) (2006) 491–502.
[38] D. Geysen, C. Vandecasteele, M. Jaspers, E. Brouwers, G. Wauters, Effect of improving flue gas cleaning on characteristics and immobilisation of APC residues from MSW incineration, Journal of Hazardous Materials 128 (1) (2006) 27–38.
[39] C.A.J. Appelo, D. Postma, Geochemistry, Groundwater and Pollution, A.A. Balkema, Rotterdam, 1994.
[40] A.K. Suryavanshi, R.N. Swamy, Stability of Friedel's salt in carbonated concrete structural elements, Cement and Concrete Research 26 (5) (1996) 729–741.
[41] J.V. Bothe, P.W. Brown, PhreeqC modeling of Friedel's salt equilibria at 23+/− 1 degrees C, Cement and Concrete Research 34 (6) (2004) 1057–1063.
[42] J.J. Dijkstra, H.A. van der Sloot, R.N.J. Comans, The leaching of major and trace elements from MSWI bottom ash as a function of pH and time, Applied Geochemistry 21 (2) (2006) 335–351.
[43] L.E. Eary, D. Rai, S.V. Mattigod, C.C. Ainsworth, Geochemical factors controlling the mobilization of inorganic constituents from fosil-fuel combustion residues 2: review of the minor elements, Journal of Environmental Quality 19 (1990) 202–214.
[44] A.M. Fallman, Leaching of chromium and barium from steel slag in laboratory and field tests – a solubility controlled process? Waste Management 20 (2–3) (2000) 149–154.
[45] A.R. Felmy, D. Rai, D.A. Moore, The solubility of (Ba,Sr)So4 precipitates – thermodynamic-equilibrium and reaction-path analysis, Geochimica et Cosmochimica Acta 57 (18) (1993) 4345–4363.
[46] J.A. Meima, A. Van Zomeren, R.N.J. Comans, Complexation of Cu with dissolved organic carbon in municipal solid waste incinerator bottom ash leachates, Environmental Science & Technology 33 (9) (1999) 1424–1429.
[47] J.J. Dijkstra, A. Van Zomeren, J.C.L. Meeussen, R.N.J. Comans, Effect of accelerated aging of MSWI bottom ash on the leaching mechanisms of copper and molybdenum, Environmental Science & Technology 40 (14) (2006) 4481–4487.
[48] A. Van Zomeren, R.N.J. Comans, Contribution of natural organic matter to copper leaching from municipal solid waste incinerator bottom ash, Environmental Science & Technology 38 (14) (2004) 3927–3932.
[49] H.A. van der Sloot, Characterization of the leaching behaviour of concrete mortars and of cement-stabilized wastes with different waste loading for long term environmental assessment, Waste Management 22 (2) (2002) 181–186.
[50] R.B. Perkins, C.D. Palmer, Solubility of Ca-6[Al(OH)(6)](2)(CrO_4)(3)·26H(2)O, the chromate analog of ettringite; 5–75 degrees C, Applied Geochemistry 15 (8) (2000) 1203–1218.
[51] M. Zhang, E.J. Reardon, Removal of B, Cr, Mo, and Se from wastewater by incorporation into hydrocalumite and ettringite, Environmental Science & Technology 37 (13) (2003) 2947–2952.
[52] J.C.L. Meeussen, ORCHESTRA: an object-oriented framework for implementing chemical equilibrium models, Environmental Science & Technology 37 (6) (2003) 1175–1182.
[53] D. Damidot, F.P. Glasser, Thermodynamic investigation of the Cao-Al_2O_3-$Caso_4$-K_2O-H_2O system at 25 degrees C, Cement and Concrete Research 23 (5) (1993) 1195–1204.
[54] R.B. Perkins, C.D. Palmer, Solubility of chromate hydrocalumite ($3CaO{\cdot}Al_2O_3{\cdot}CaCrO_4{\cdot}n$H(2)O) 5–75 degrees C, Cement and Concrete Research 31 (7) (2001) 983–992.
[55] A. Kindness, E.E. Lachowski, A.K. Minocha, F.P. Glasser, Immobilization and fixation of molybdenum(Vi) by portland-cement, Waste Management 14 (2) (1994) 97–102.
[56] J.V. Bothe, P.W. Brown, The stabilities of calcium arsenates at 23+/- 1 degrees C, Journal of Hazardous Materials 69 (2) (1999) 197–207.
[57] Y.N. Zhu, X.H. Zhang, Q.L. Xie, Y.D. Chen, D.Q. Wang, Y.P. Liang, J. Lu, Solubility and stability of barium arsenate and barium hydrogen arsenate at 25 degrees C, Journal of Hazardous Materials 120 (1–3) (2005) 37–44.
[58] C.A. Johnson, H. Moench, P. Wersin, P. Kugler, C. Wenger, Solubility of antimony and other elements in samples taken from shooting ranges, Journal of Environmental Quality 34 (1) (2005) 248–254.